Biophysical Journal, Volume *114*

Supplemental Information

Molecular Mechanisms of Tight Binding through Fuzzy Interactions

Qingliang Shen, Jie Shi, Danyun Zeng, Baoyu Zhao, Pingwei Li, Wonmuk Hwang, and Jae-Hyun Cho

Table S1. X-ray diffraction and refinement statistics for nSH3-PRM^{NS1} complex.

	6ATV.PDB
Data collection	
Space group	$P6_122$
Cell dimensions	
a, *b*, *c* (Å)	39.84, 39.84, 171.95
α, β, γ (°)	90.0, 90.0, 120.0
Resolution (Å)	1.75 (1.78 to 1.75)
R_{merge}	10.2% (23.3%)
$I / \sigma I$	16.8 (3.5)
Completeness (%)	94.9 (67.0)
Redundancy	12.0 (3.3)
Refinement	
Resolution (Å)	1.75
No. Reflections	8437
R_{work}/R_{free}	0.184/0.205
No. atoms	721
Protein	493
Ligand	114
Water	114
B-factors	
Protein	18.8
Ligand	18.8
Water	32.8
r.m.s. deviations	
Bond lengths (Å)	0.006
Bond angles (°)	0.781

* Values in parentheses are for the highest-resolution shells.

Table S2-1. The difference in average pairwise distances.

Residues in PRM^{NS1}	Difference in average pairwise distances (MD[a] - Crystal[b]) (Å)					
	Acidic residues in nSH3 domain					
	D142	D147	E149	D150	D163	E166
R211	0.0	-[c]	-[c]	-[c]	-[c]	-[c]
K219	-[c]	1.5	1.3	0.5	-0.2	0.7
R220	-[c]	-1.4	-1.3	-2.6	-5.4	-5.4
K221	-[c]	-1.3	1.8	-0.0	2.6	-0.5

[a]MD trajectories of PRM^{NS1A}
[b]Crystal structure of PRM^{NS1A} (PDB ID: 5UL6)
[c]These distances were longer than 15 Å and not included in the analysis.

Table S2-2. The difference in average pairwise distances.

Residues in PRM^{NS1}	Difference in average pairwise distances (MD[a] - Crystal[b]) (Å)					
	Acidic residues in nSH3 domain					
	D142	D147	E149	D150	D163	E166
R211	-1.7	-[c]	-[c]	-[c]	-[c]	-[c]
K219	-[c]	-6.1	-4.0	-4.9	1.9	-1.6
R220	-[c]	-0.6	0.5	1.1	3.2	0.9
K221	-[c]	-5.6	-3.6	-3.0	5.0	-0.3

[a]MD trajectories of PRM^{NS1B}
[b]Crystal structure of PRM^{NS1B} (PDB ID: 6ATV)
[c]These distances were longer than 15 Å and not included in the analysis.

Figure S1

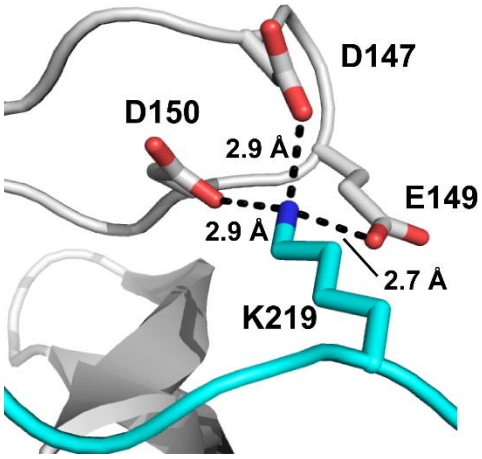

Figure S1. (A) The complex contains short-range electrostatic interactions between K217 of PRM^{NS1} and three acidic residues (D147, E149, and D150) in the nSH3 domain (PDB ID: 6ATV). The distances in the figure were measured between N^{ζ} of K219 and $O^{\delta/\varepsilon}$ of the acidic residues.

Figure S2

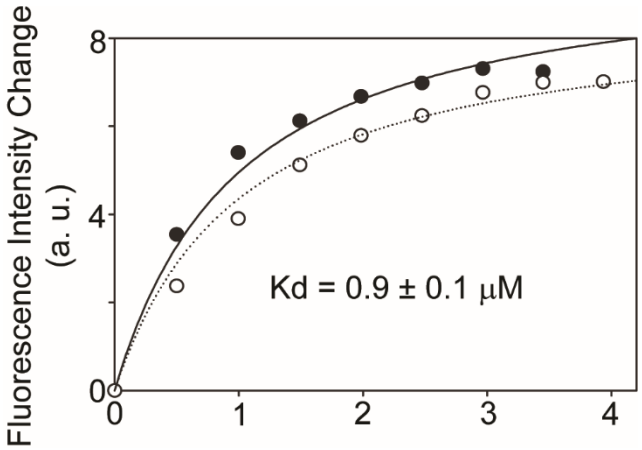

Figure S2. Fluorescence-based measurement of binding affinity between the nSH3 domain and mutant PRM^{NS1}, in which three C-terminal positively charged residues (K219-R220-K221) are replaced by Gly. The K_d value is from two repeated measurements.

Figure S3.

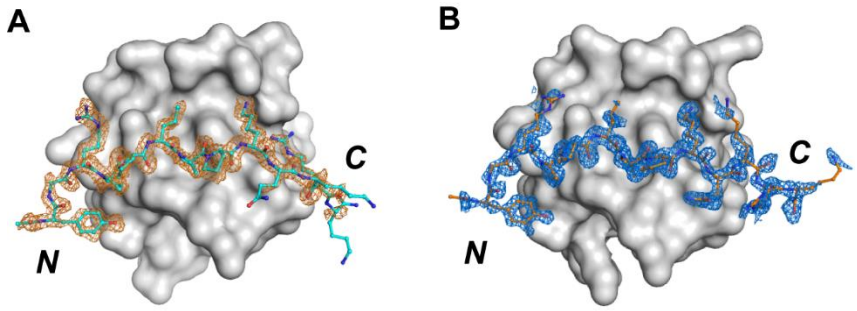

Figure S3. σA weighted $F_o - F_c$ map (contoured at 2σ) of (A) PRM^{NS1B} and (B) PRM^{NS1A}.

Figure S4.

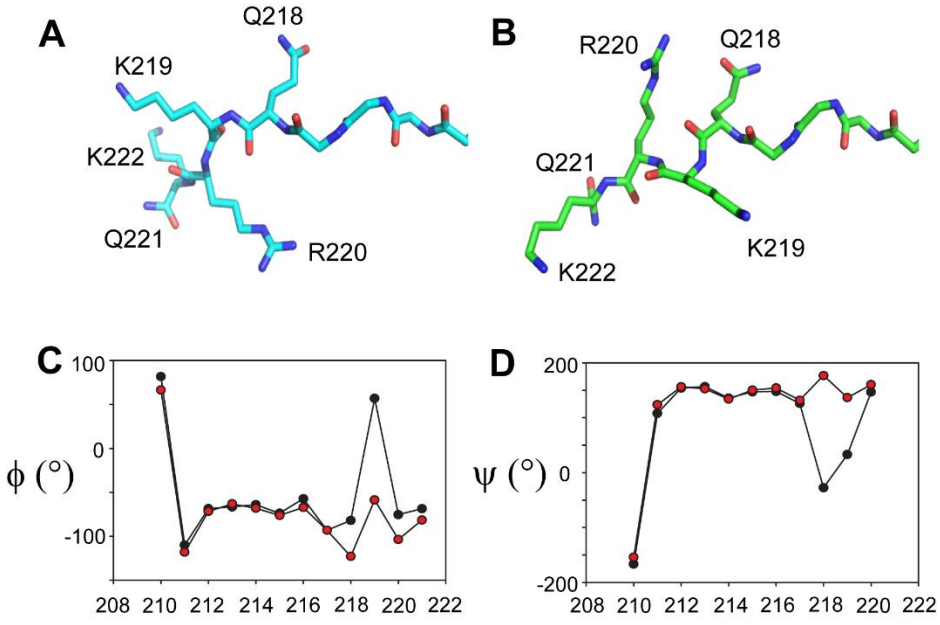

Figure S4. Conformational difference in the C-terminal region of the bound (A) PRM^{NS1B} and (B) PRM^{NS1A}. Significant changes in backbone (C) ϕ and (D) ψ angles of Q218 induced large changes in the conformations of positively charged residues in the C-terminal end of Q218.

Figure S5

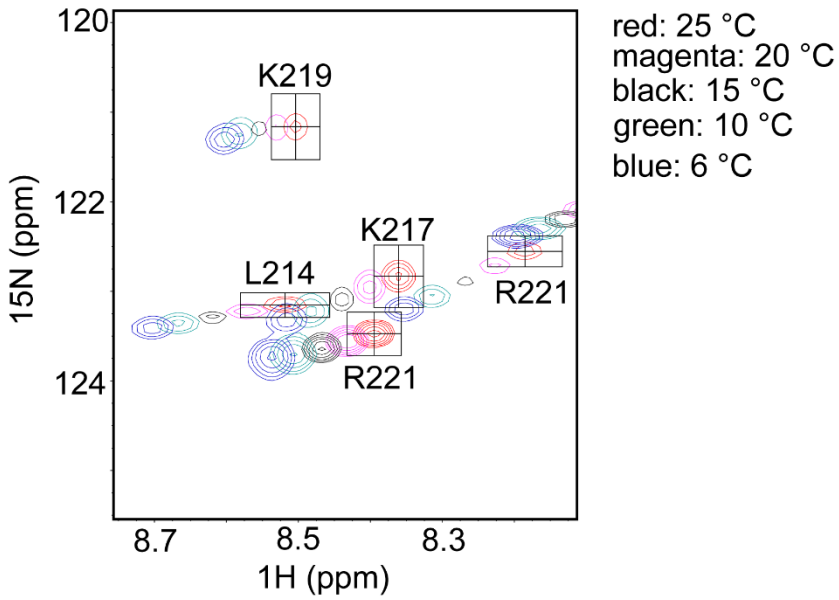

Figure S5. An overlay of temperature-dependent chemical shift changes for the C-terminal positively charged residues (K217, K219, R220, and K221) in PRM^{NS1}.

Figure S6

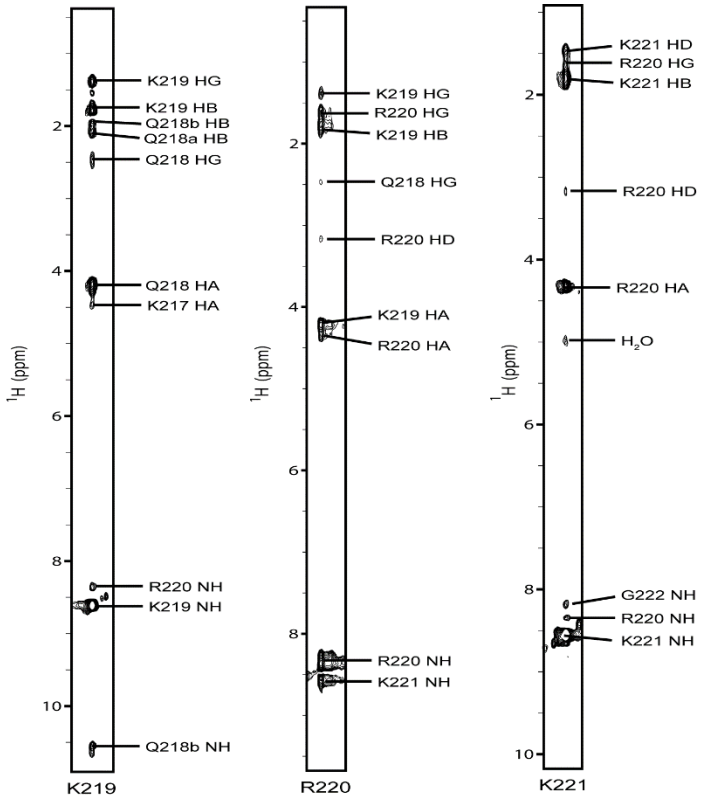

Figure S6. ^{15}N-edited NOESY HSQC of the C-terminal positively charged residues (K219, R220, and K221) in PRM^{NS1} bound to the nSH3 domain. The data was acquired using a sample of ^{15}N-labeled PRM^{NS1} saturated by non-labeled nSH3 domain. The NOESY mixing time was 100 ms.

Figure S7

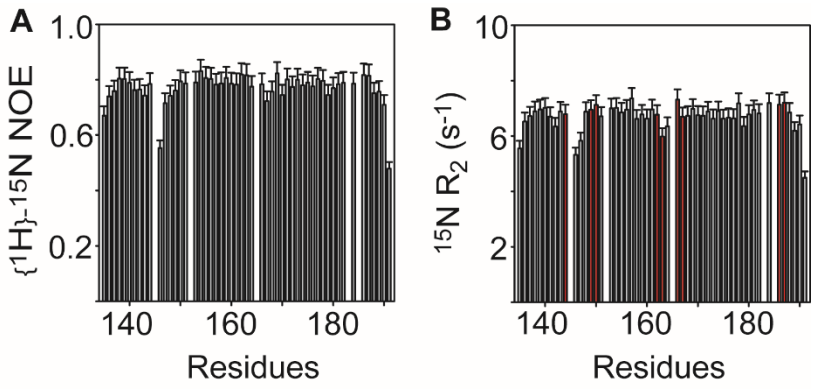

Figure S7. (A) {^{1}H}-^{15}N heteronuclear NOE and (B) ^{15}N R_2 of the nSH3 domain saturated by PRM^{NS1}. Red bars represent the residues in the nSH3 domain that are in the binding interface with PRM^{NS1}. This represents that the elevated R_2 in PRM^{NS1} is not induced by its on-off process.